

The Telecoupling GeoApp: A Web-GIS Application to Systematically Analyze Telecouplings and Sustainable Development

Paul McCord^a, Francesco Tonini^a, Jianguo Liu^a

^a Center for Systems Integration and Sustainability, Michigan State University, East Lansing, MI, USA

Abstract

Global challenges, such as chronic hunger in developing and developed regions, loss of wildlife habitat, and the continuing rise of greenhouse gas emissions from human activities, can be addressed only through an integrated approach. The telecoupling concept is one such approach: it explores socioeconomic and environmental interactions among coupled human-natural systems over distances. The telecoupling framework is therefore well-positioned to provide new insights to persistent global sustainability challenges. To operationalize the framework, we have developed the Telecoupling GeoApp, a new web-based component of the Telecoupling Toolbox that provides researchers and practitioners with a useful platform to address globally important issues such as international trade, species invasion, biodiversity conservation, and land-use change. The *GeoApp* features mapping and geospatial analysis tools to visualize and quantify the five major interrelated components of the telecoupling framework (systems, flows, agents, causes, and effects). In this paper, we demonstrate the GeoApp's functionality by applying it to a case study in which distant systems interact across space and time: the Brazil-China soybean telecoupling. We conclude by highlighting the advantages of the Telecoupling GeoApp in addressing global sustainability challenges. It is our hope that this web application will be valuable to a range of users exploring telecouplings and outcomes across distant coupled human-natural systems for achieving sustainable development goals.

Keywords: CHANS, land-use change, sustainable development, telecoupling, international trade, webGIS

1. Introduction

The world is increasingly connected through flows of materials and information across vast distances, the emergence of new networks linking actors, and the presence of spatial externalities joining localized processes to global systems (Foley et al., 2005; Peters et al., 2008; Liu et al., 2015a). These interconnections can be beneficial: sustainable globalized food systems can improve food security (Godfray et al., 2010), cell phone proliferation and short message services offer remote rural farmers valuable climatic and planting information (Singels and Smith, 2006; Car et al., 2012), and tourism and trade potentially allow ecosystem services to be provided to areas where the supply of such services fails to meet demand (Zeppel, 2008; Liu et al., 2016). Yet increased connectivity may also result in greater damage to global systems from human activities due both to anthropogenic manipulation of geophysical processes, e.g., climate change, and the accumulation of environmental damage at multiple discrete sites, e.g., biodiversity loss and land use change (Vitousek, 1992; Stern, 2008; Vörösmarty et al., 2010; Dou et al., *in press*). These processes of global environmental change - and the human dimensions of such change - have been well-documented (e.g., Turner et al., 1990; Geist and Lambin, 2002; Turner et al., 2007; DeFries et al., 2010; Lambin and Meyfroidt, 2011; Adger et al., 2013; Kramer et al., 2017).

Concern about the effects and implications of global environmental change as well as efforts to better understand how to meet humanity's needs while maintaining the integrity of environmental systems led to the field of sustainability science (Kates et al., 2001). Fundamentally, global sustainability (and the obstacles posed to it) is shaped by complex and multi-scale human-environment interactions (Turner et al., 2003; Komiyama and Takeuchi, 2006; Liu et al., 2015a). Many efforts have emerged to understand these interactions and to assess progress toward global sustainability. For instance, the Sustainable Development Goals, adopted by the United Nations (UN) General Assembly in 2015, provide a set of seventeen global goals and targets for all countries, including goals related to addressing climate change and sustainably using terrestrial and aquatic resources (Sachs, 2012; United Nations, 2016). Other efforts to confront global sustainability challenges have included crafting frameworks to investigate the components, processes, and multi-scalar dimensions of sustainability topics (e.g., Millennium Ecosystem Assessment, 2005; Ostrom, 2009), frameworks to interrogate the vulnerability of coupled human-natural systems (e.g., Turner et al., 2003; Polsky et al., 2007), and frameworks particularly oriented toward understanding system interactions across space (Liu et al., 2013; Liu et al., 2015b, Liu, 2017).

The telecoupling framework, which we focus on in this paper, was developed to provide an integrated understanding of socioeconomic and environmental interactions between coupled human and natural systems over distances (Liu et al., 2013). The framework consists of five interrelated components: coupled human and natural systems; flows between systems, which can

include flows of materials, energy, and information, among others; agents enabling flows; causes behind the flows; and the effects of interactions. Systems are classified as either a sending system (e.g., resource exporter), a receiving system (e.g., resource importer), or a spillover system (e.g., a country that is affected by trade between the sending and receiving systems).

Multiple studies have employed the telecoupling framework to analyze various components of distant socioeconomic and environmental interactions (e.g., Carter et al., 2014; Liu, 2014; Liu et al., 2015*b*; Deines et al., 2016; Gasparri et al., 2016; Silva et al., 2017; Sun et al., 2017). To support this research, a suite of desktop-based software tools have been developed to allow researchers to operationalize the framework and systematically explore complex interactions (Tonini and Liu, 2017). Following the deployment of these desktop-based tools, the next step has been to develop a web-based application to provide greater flexibility in visualizing and quantifying telecoupling components and their outcomes.

This paper introduces the Telecoupling GeoApp (hereinafter, the GeoApp), a web-based application that operationalizes the telecoupling framework through a suite of spatially explicit geoprocessing tools while avoiding desktop-based software installation procedures and licenses. In this way, the GeoApp is an example of a web GIS application where a range of simple-to-complex mapping and geospatial analysis operations can be completed with the primary preconditions being an internet connection and a modern browser (Fu and Sun, 2010). It offers a fully interactive platform to explore the systems, flows, agents, causes, and effects of a telecoupling. To demonstrate its functionality, we apply the GeoApp to a case study with global sustainability implications: the Brazil-China soybean telecoupling wherein Brazil exports millions of tons of soybeans to China every year (more than 30 million metric tons were exported in 2014; see Silva et al (2017)). It is our hope that this web application will be valuable to a range of users exploring various telecouplings and outcomes between distant systems.

2. The Telecoupling GeoApp

2.1. The Telecoupling Toolbox

The GeoApp is part of a larger collection of software tools and applications called the Telecoupling Toolbox (Tonini and Liu, 2017). At present, the Telecoupling Toolbox consists of two main products: the ArcGIS Toolbox and the GeoApp. The ArcGIS Toolbox features a collection of custom geoprocessing tools to be used with ESRI's ArcGIS Desktop, while the GeoApp offers a dynamic, interactive web GIS platform along with a large collection of mapping and analysis tools to systematically study telecoupling.

Both the GeoApp and the ArcGIS Toolbox have been developed in a modular fashion to facilitate the integration with existing third-party tools, e.g. InVEST (Kareiva et al. 2011; Sharp et al. 2017), and to accommodate the development of custom tools and models as the demand for additional telecoupling applications grows. In order to maintain transparency and promote collaborations between users from different fields, all source code, sample data, and documentation of all tools and applications within the Telecoupling Toolbox are freely available and hosted on a public online repository: <https://msu-csis.github.io/telecoupling-toolbox/>.

2.2. Design of the Telecoupling GeoApp

The Telecoupling GeoApp (<https://telecoupling.msu.edu/geo-app>) is customized using one of ESRI's Web AppBuilder Developer Edition templates and deployed on Amazon Web Services (AWS), a compute-friendly environment that enables efficient data management and analysis at scale (Amazon AWS, 2017). The same virtual server is used as both the web application tier and the GIS web service tier for storing and serving public-facing geoprocessing services. An Elastic Load Balancing (ELB) service is set up along with auto scaling to automatically route incoming web traffic across a changing number of Elastic Compute Cloud (EC2) instances that increase or decrease based on user demand (Figure 1).

The GeoApp is designed for a broad audience of researchers from many disciplines interested in applying the telecoupling framework. Unlike the ArcGIS Toolbox, the GeoApp requires only an internet connection and a modern web browser to be used. Users do not need to purchase any proprietary software license, nor do they have to spend time installing the necessary libraries for the tools to work on a desktop environment. The application offers an intuitive and user-friendly web interface that enhances the overall user experience. Specifically, users do not have to be proficient in a given software platform to understand and use the GeoApp.

Similar to the ArcGIS Toolbox, the GeoApp is *spatially explicit* to map and represent the five main components of the telecoupling framework (systems, agents, flows, causes, effects), as well as *multiscale* in that users can define the spatial scale of analysis ranging from the parcel to entire regions, countries, continents, and the globe if appropriate. Moreover, the GeoApp is modular to allow the integration of existing tools and models to assess synergies and tradeoffs associated with policies and other local-to-global interventions on issues such as land use and land cover change, species invasion, migration, flows of ecosystem services, and international trade of goods and products.

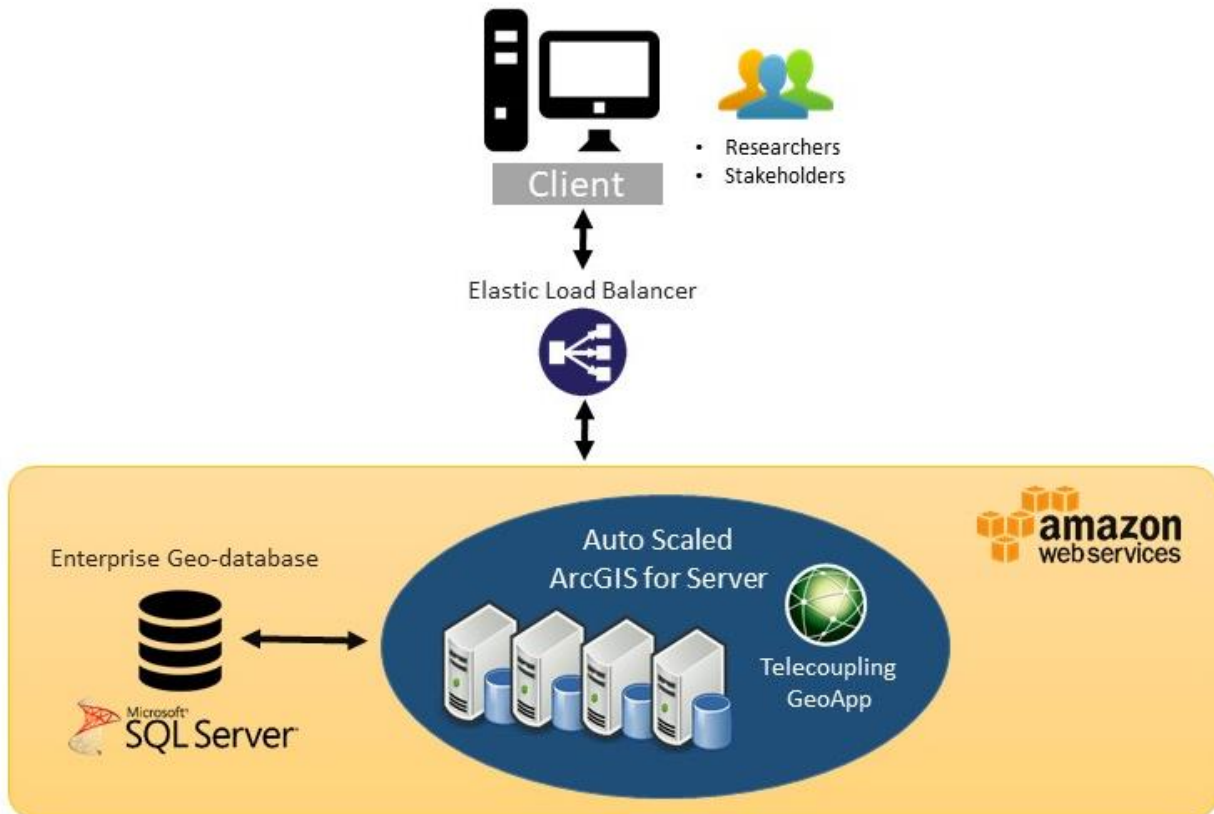


Figure 1. Architecture of the Telecoupling GeoApp deployment with ArcGIS Server on Amazon Web Services (AWS). Users (researchers, stakeholders) interact with the GeoApp via a computer and a modern browser. Behind the scenes, the Amazon Elastic Load Balancer (ELB) directs incoming and outgoing traffic between the client and the Amazon cloud servers. Both the web server hosting the GeoApp and the ArcGIS Server site are hosted on the same virtual server. The ArcGIS Server site is load-balanced with auto scaling to automatically route incoming web traffic across a changing number of Elastic Compute Cloud (EC2) instances that increase or decrease based on user demand. Data behind the GeoApp are pulled from an enterprise geo-database in Microsoft SQL Server.

2.3. Structure of the Telecoupling GeoApp

The Telecoupling GeoApp includes a large collection of widgets dedicated to separate tasks such as querying data, mapping and visualization, quantitative analysis, and satellite imagery analysis (Figure 2). We chose to group widgets and their corresponding tasks by their purpose. Therefore, widgets with a general purpose (mapping and visualization, query and selection) are separate from the telecoupling analysis and imagery analysis categories, even if these include their own visualization or data querying tasks.



TELECOUPLING GEOAPP

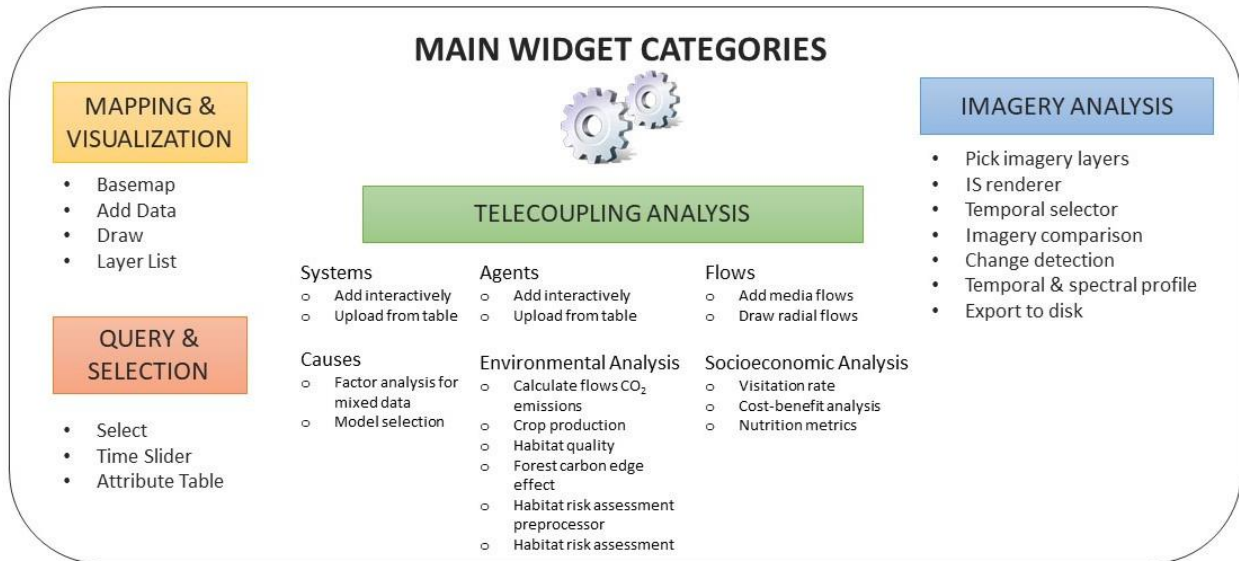


Figure 2. Main widget categories and tasks found within the Telecoupling GeoApp. The telecoupling analysis category includes a mix of widgets and tasks that are either qualitative (systems, agents, flows) or quantitative (causes, environmental analysis, socioeconomic analysis). Similarly, the imagery analysis widget includes a mix of querying/visualization tasks (pick imagery layers, image service (IS) renderer, temporal selector, imagery comparison, temporal and spectral profile), quantitative tasks (change detection), and administrative tasks (export to disk).

2.3.1 Mapping and visualization

Mapping and visualization widgets include simple tasks such as switching basemap type on-the-fly, drawing shapes and text annotations on top of the map, toggling on/off operational layers that are either included with the GeoApp by default or produced as output from other widgets, and finally adding data (spatial or tabular) from the user's local computer or an openly available collection of GIS layers from ESRI's Living Atlas of the World (ESRI, 2017). This way, users have the opportunity to add any additional layers that are deemed important to inform their analysis and provide more context.

2.3.2 Query and selection

Query and selection widgets include a traditional *select* task, where users can select a subset of objects from the map, a time slider for slicing and subsetting layers that have a temporal attribute attached to them, and querying of records directly from the attribute table associated with a layer. The time slider can be particularly helpful for focusing the attention on specific temporal

windows of a given mapped quantity and improve the understanding of potential hidden patterns prior to the analysis.

2.3.3 Imagery Analysis

The imagery analysis widgets are slightly customized versions of ESRI's publicly available Web AppBuilder for Image Services 2.0 online collection (<https://github.com/Esri/WAB-Image-Services-Widgets>). The imagery widgets available within the GeoApp offer users a way of exploring a vast collection of satellite imagery. The IS renderer - or image service renderer - widget lets users select a different spectral band combination from a pre-defined list of widely used field applications (e.g. agriculture, water, etc.). Changing band combination helps isolate specific natural or built environment features that users are most interested in. The temporal selector widget is similar to the time slider within the query and selection category but it only works with satellite imagery collections. Other widgets such as temporal and spectral profile or image comparison serve as additional tools to explore and identify change occurring across space and time, thus offering potential qualitative insight of the local effects from a particular telecoupling process on the natural or human environment. At present, the change detection widget is the only quantitative tool that can actually compute and map the difference between two chosen images. These differences can be expressed in terms of absolute values or pre-defined subsets of indicators like the Normalized Difference Vegetation Index (NDVI), which employs different spectral bands to indicate the presence of healthy green vegetation, or Soil Adjusted Vegetation Index (Huete, 1988), Water Index (McFeeters, 1996), or Burn Index (Kasischke et al., 2008). Finally, the export to disk widget allows the user to save a given image locally.

2.3.4 Telecoupling Analysis

The telecoupling analysis widgets represent the core of the GeoApp and were developed specifically to help users map and quantify relationships and connections between natural and human systems under the telecoupling framework. Four of the main components of the framework (systems, agents, flows, causes) are each represented by their own separate widget in the GeoApp. The *effects* component is split into the environmental analysis and socioeconomic analysis widgets for clarity and to avoid cluttering of geoprocessing tasks that would otherwise occur within a single widget. Moreover, using the more generic term "analysis" rather than simply "effects" conveys the concept that some of the tools included in the two widget groups can be used to spatially analyze environmental or socioeconomic processes that, in the terminology of the telecoupling framework, are both causes and effects depending on the processes and interactions being investigated. At present, the systems, agents, and flows widgets are mostly qualitative and should be used for mapping and visualization purposes, though we plan to build more quantitative capabilities into future flows widgets. Users can use these tasks to assign a spatial location to all telecoupling systems, agents, and draw flow lines that connect systems to show transfer of materials or energy between pairs of locations. The tasks within the

causes widget offer users statistical methods such as factor analysis for mixed data in order to separate and identify potential factors involved in the observed connections between telecoupled systems. The bulk of the geoprocessing tasks are found within both the environmental and socioeconomic analysis widgets, with several widgets linking to third-party InVEST 3.3.3 models (Sharp et al., 2017). Here, users can quantify impacts on pre-defined areas of interest that relate to ecosystems services like habitat quality, carbon stock, crop production, environmental pollution in terms of emitted CO₂, or economic profits/losses, change in visitation rate of tourists, or nutritional demand given information on the local population.

3. Applications of the Telecoupling GeoApp

In this section we demonstrate the GeoApp's functionality by applying it to the Brazil-China soybean telecoupling. First, we provide a contextual background of this telecoupling. We then use the GeoApp to explore outcomes, including changes in land use and land cover, from these interconnections and relate the insight provided from these analyses to several indicators of sustainable development provided by the UN. All of the widgets used in these analyses can be found in either the *telecoupling analysis* or *imagery analysis* category from Figure 2.

3.1. The Brazil-China Soybean Telecoupling

China domesticated soybeans more than 3,000 years ago (Sun et al., 2015), but became a net importer of soybeans for the first time in the mid-1990s. In 2003 it passed the European Union as the largest soybean importer in the world (Tuan et al., 2004). This rapid transition from net soybean exporter in the early 1990s to the world's largest importer over the course of a single decade was propelled by several forces, including trade liberalization, the growth of the Chinese middle class, and shifting dietary habits (Nepstad et al., 2006; Silva et al., 2017). Of particular note in this transition is China's accession to the World Trade Organization (WTO) in 2001 wherein China agreed to a range of market access obligations concerning, among others, agricultural goods. Hence, the country's agricultural sector was exposed to international trading and competition. Since joining the WTO, China's soy imports have increased from roughly 15 million tons to over 70 million tons in 2014 (Silva et al., 2017), with approximately half of all soybean imports coming from Brazil.

Brazilian soybean production spiked in the 1970s due largely to commercialization of low-latitude varieties and a global price increase in protein meals (Warnken, 1999; Goldsmith, 2008). By the middle of the 1970s, Brazilian soybean production surpassed that of China making Brazil the world's second largest soybean producer, trailing only the United States (FAO, 2017). As

production became increasingly oriented toward export markets and regions experienced economic development, land previously on Brazil's frontier, particularly in the Amazon and Cerrado biomes, grew more desirable for production (Morton et al., 2006; DeFries et al., 2010; Lambin and Meyfroidt, 2011). Since the late 1990s, Brazil's soybean expansion has been fueled by a combination of demand- and supply-side drivers. On the supply-side, attention has been given to efforts to bring new land under production, development of port and road infrastructure, and policies to attract human and financial capital (Brannstrom et al., 2008; Richards et al., 2012). However, the present analysis is primarily concerned with the demand-driven effects of soybean export to China, which, as mentioned above, has swelled as a result of trade liberalization and expansion of China's middle class.

Silva et al. (2017) identified a 1668% increase in soybean production in Brazil's Tocantins state from 2000 to 2015, stimulated largely by Chinese demand. In fact, in 2015 36% of Tocantins' production was exported to China, with the remainder either exported to other countries (28%) or consumed domestically (36%). Similarly, Silva et al. found that 37% of soybean production in 2016 within the state of Goiás was destined for foreign markets, and of this, 78% was sent to China. In the remainder of this section, we use the GeoApp to explore outcomes of Brazilian soybean expansion within yet another state that has experienced dramatic land cover transformation: Mato Grosso. In an effort to acknowledge the ecological impacts of this soybean expansion, we have chosen to focus on a time point and spatial location where previous research has identified the direct conversion of land cover from forest to cropland. Morton et al. (2006) identified locations in the southern Brazilian Amazon where forests directly gave way to agriculture from 2001 to 2004. The authors further correlated this deforestation with international soybean prices establishing a connection between land conversion in Mato Grosso and soybean demand from global markets. While we do not have data on where soy produced in this area of interest was sent, we are confident that foreign demand from China played a significant role given the country's emergence as a major international player at this time. We depict the flow of soybeans from Mato Grosso to the ten largest Chinese cities in terms of population using the GeoApp's Draw Radial Flows widget in Figure 3.

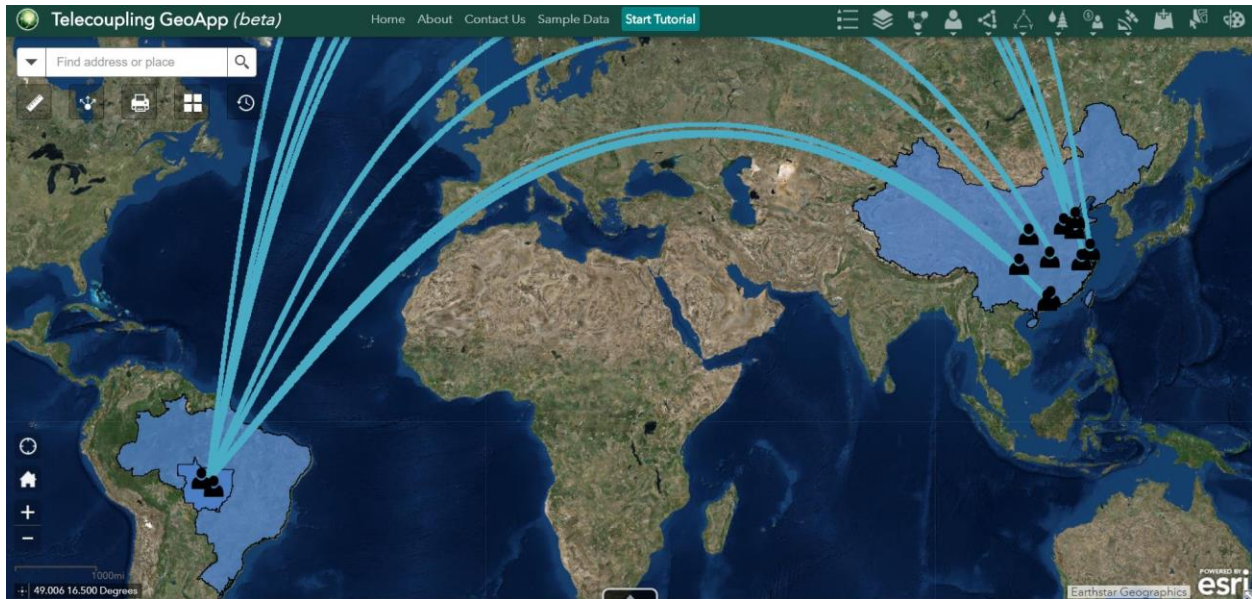


Figure 3. Screenshot of GeoApp depicting the flow of soybeans from Mato Grosso to China, as well as agents in the sending system (two agent icons were added to simply indicate that large-scale and small-scale farmers are dominant actors in Mato Grosso) and agents in the receiving system (one agent icon was added for each of the ten largest Chinese cities). *Note:* This image was produced using the GeoApp’s Draw Radial Flows and Add Agents tools. The origin of the flows is drawn from Sinop, Brazil, while the destinations are the ten largest Chinese cities in terms of population. We recognize that soy commodities are typically transported by sea; however, at the moment, the depiction of flows with the GeoApp must be visualized radially.

3.2. Methods

We now identify an area of interest that has undergone significant change as a result of expanding soybean production. The GeoApp will be applied to explore this area’s land cover change, transformations in agricultural productivity, alterations to carbon stock, and species habitat risk; all of which are outcomes fueled by interactions between Brazilian soybean production and international demand, primarily demand from Chinese markets (Figure 4). This area of interest will hereinafter be referred to as *AOI*. Note that the widgets employed to investigate carbon stock, species habitat risk, and agricultural productivity within the *AOI* link to InVEST 3.3.3 models. For a full explanation of the procedures and equations used by each InVEST model, the reader is encouraged to consult the official documentation provided by the NatCap project (see Sharp et al., 2017).

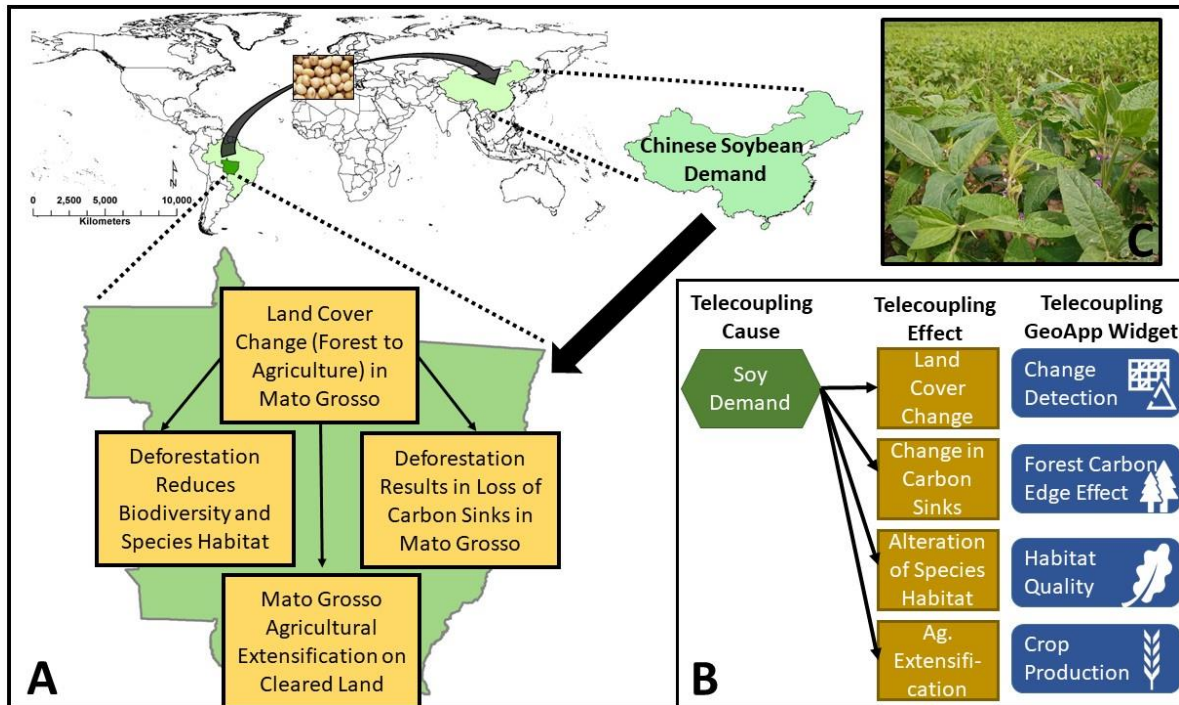


Figure 4. Soybean demand from China results in a range of outcomes, including land cover change, species habitat quality and biodiversity loss, fluctuations in carbon storage, and agricultural extensification (A). GeoApp widgets exist to investigate each of these outcomes (B). Soybeans in Mato Grosso (C), photo credit: Yue Dou (July, 2017).

3.2.1. The Area of Interest: Agricultural Expansion in Mato Grosso, Brazil

The AOI is shown in Figure 5, and it is the same region in central Mato Grosso state from Morton et al. (2006) that occupies approximately 235,580 km². Morton et al. (2006) focused on this region to identify large forest clearings to make way for cropland from 2001 to 2004. Additionally, the authors correlated these land cover changes with mean annual soybean prices. Mato Grosso state experienced the highest rate of deforestation and soybean production over the 2001 to 2004 period; thus, in the context of the Brazil-China soybean telecoupling, it is a logical region to focus on within the sending system.

In order to create spatially explicit zones of agricultural expansion within the AOI, we utilized findings from Morton et al. (2006) in which the authors published a map isolating areas deforested and converted to cropland over the 2001 to 2004 period. This map featured identifiable reference points, which we used to georeference the map in ArcMap 10.5. Once the map was georeferenced, we digitized all areas identified by Morton et al. (2006) as “cropland deforestation” clearings. In so doing, we created a collection of spatially explicit polygons within which we used the GeoApp to explore changes to land cover, carbon stock, species habitat, and agricultural productivity (see Figure 5).

3.2.2. Land Cover Change

Table 1 indicates the data inputs and outputs for each GeoApp widget demonstrated herein. Land cover change within the AOI was investigated using the GeoApp's Change Detection widget. We used a Landsat image from December 31, 2004 as the model's primary image (i.e., the most recent image). This image was chosen because it represents a time point at the conclusion of the Morton et al. (2006) analysis period. As the secondary image (i.e., the earlier of the two images), we used Landsat data from December 31, 1999. This image was chosen because it was taken before the Morton et al. (2006) analysis period and captured the same season as the primary image, thus minimizing differences from normal plant life cycles. Figure 6 displays the primary and secondary Landsat images. The change detection image was created by finding the difference between NDVI values – constructed from the images' infrared and red bands – to identify locations of increased vegetative cover (i.e., locations where pixel values from the 2004 image were greater than those from 1999) and locations of decreased vegetative cover (i.e., locations where pixel values from the 1999 image were greater than those from 2004). The resulting change detection image is presented in the Results section.

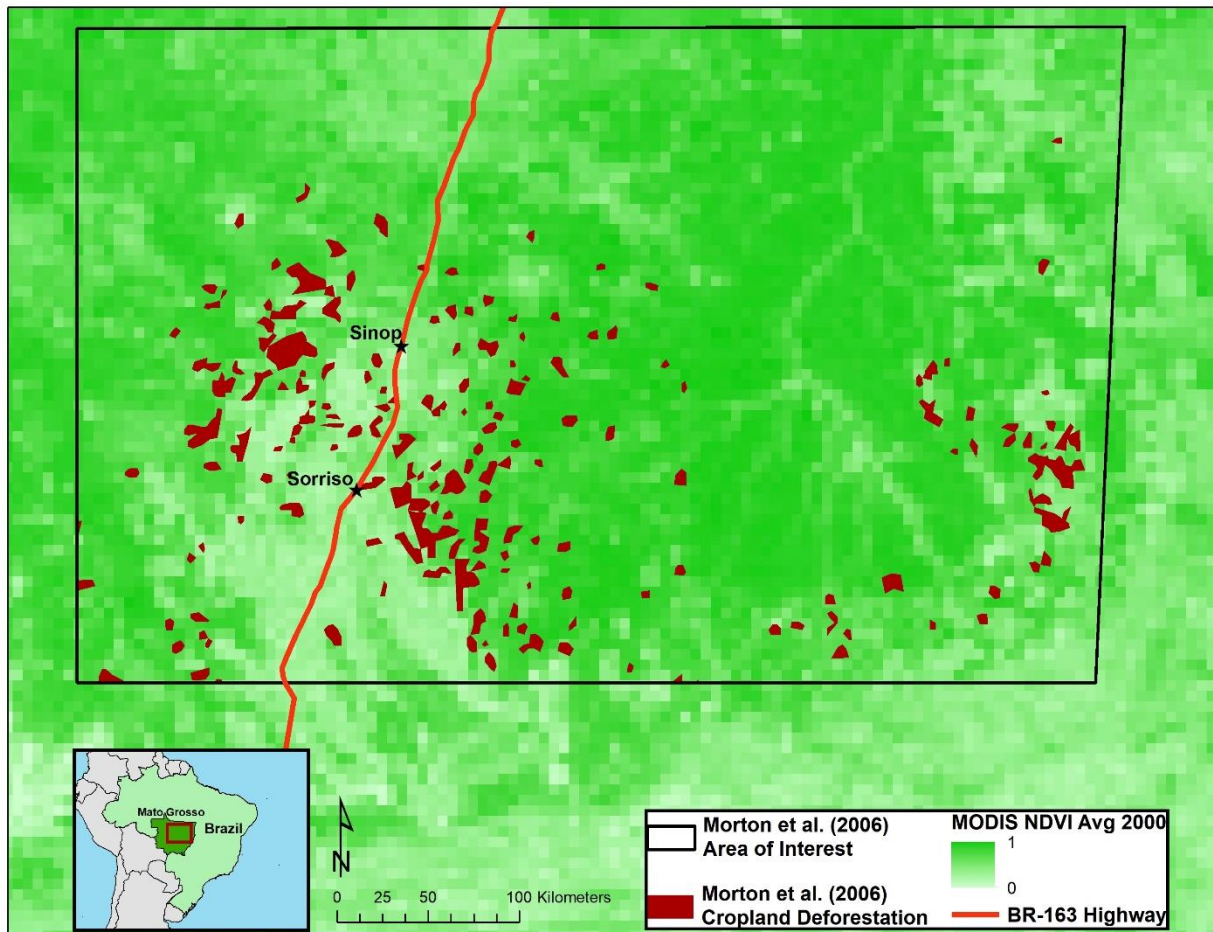


Figure 5. The Area of Interest. This area of interest is the same as that explored by Morton et al. (2006). Cropland deforestation sites are shown in dark red.

3.2.3. Forest Carbon Edge Effect

Above-ground carbon storage that was lost as a result of agricultural land conversion within the AOI was calculated using the GeoApp's Forest Carbon Edge Effect widget (see Table 1 for a general description of model inputs and output). We used a 2000 land cover image to identify forested and non-forested areas. This image was obtained from the *MapBiomass Project*, a multi-institutional initiative to generate annual land cover and land use maps using automatic classification processes applied to satellite images (a complete description of the project can be found at <http://mapbiomas.org>). Carbon stored within forested cells were estimated using pre-generated values from Chaplin-Kramer et al. (2015). Non-forest carbon density values relevant to the AOI were obtained from Fernside (1997) and Miranda et al. (2014a) and were provided to the model in a CSV file.

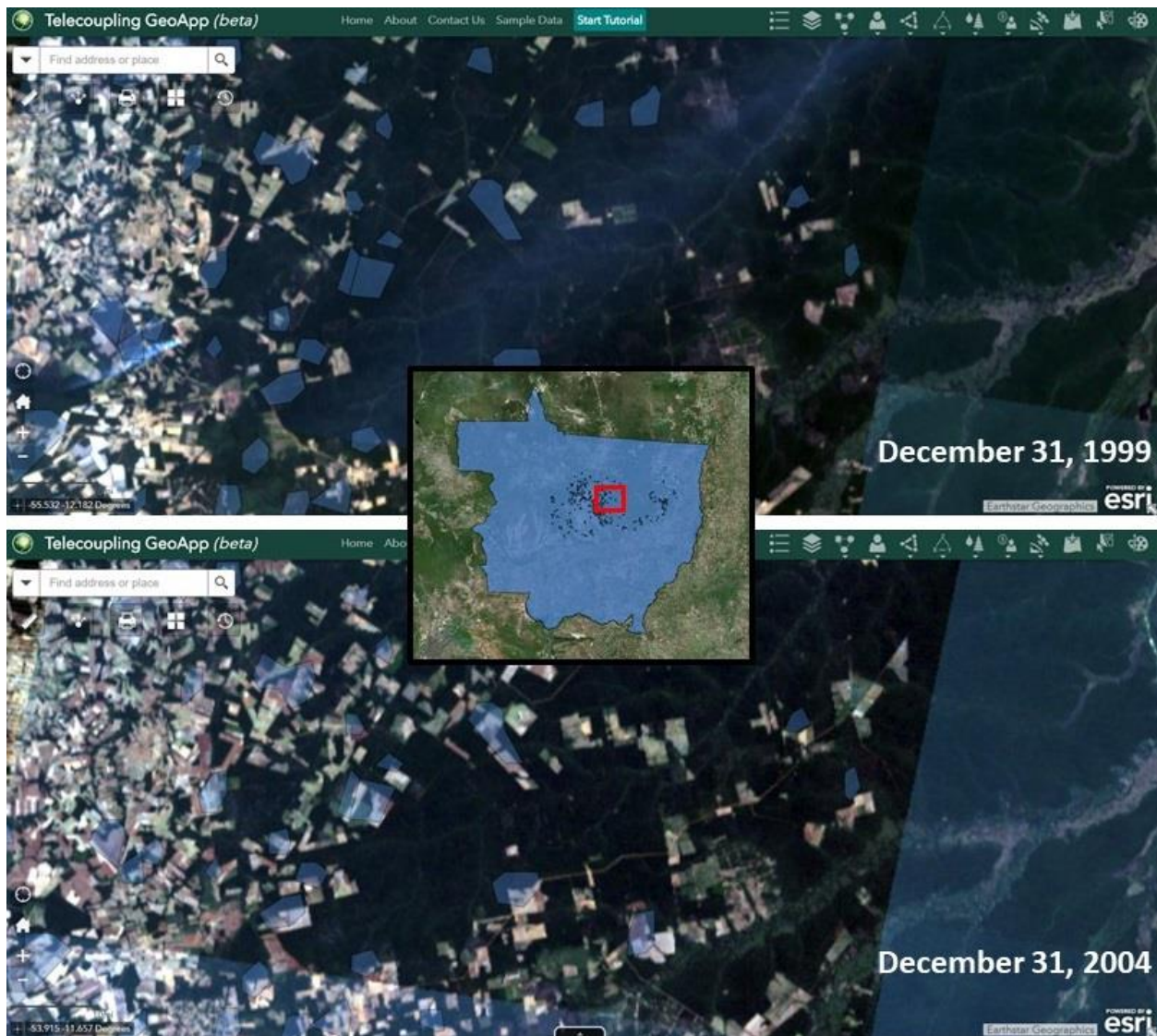


Figure 6. The primary (December 31, 2004) and secondary (December 31, 1999) images included in the change detection analysis. The cropland deforestation sites from Morton et al. (2006) are included at 50% transparency to facilitate image comparison.

Table 1

Model inputs and analysis procedures for select GeoApp widgets.

Widget Name	Inputs	Analysis Procedure and Output
Change Detection	<ul style="list-style-type: none"> • Primary remotely sensed image (i.e., the more recent image). • Secondary remotely sensed image (i.e., the earlier image). 	<ul style="list-style-type: none"> • Both primary and secondary image must overlap. • The tool produces an image indicating areas of increased or decreased vegetation.
Forest Carbon Edge Effect (see Chaplin-Kramer et al., 2015; Sharp et al., 2017 for detail)	<ul style="list-style-type: none"> • Land cover raster of the area of interest. • CSV file indicating which classes from the land cover raster are forest, and the carbon density (in Mg/ha) for non-forest classes. • User must indicate if all carbon pools are to be calculated, or if it is limited to only above-ground pools. 	<ul style="list-style-type: none"> • The tool applies information from the CSV file to the land cover classifications to calculate carbon pools. • The tool produces a raster of carbon stock (in Mg) per pixel.
Habitat Quality (see Sharp et al., 2017 for detail)	<ul style="list-style-type: none"> • Land cover raster of the area of interest. • Raster(s) indicating the presence or absence of threats to the species of interest (e.g., road networks, human settlements). • CSV file of each threat's relative importance and impacts across space. • CSV file indicating which classes from the land cover raster should be considered habitat. 	<ul style="list-style-type: none"> • Habitat quality and species risk are assessed using the presence of threats, their influence on species well-being, and the proximity of species habitat to threats. • The tool produces two rasters, one of relative habitat quality on a scale of 0 to 1, and the other of relative habitat degradation on a scale of 0 to 1.
Crop Production (see Monfreda et al., 2008; Mueller et al., 2012; Sharp et al., 2017 for detail)	<ul style="list-style-type: none"> • A "Crop Management Scenario" raster that indicates the cells of crop production within the area of interest. • CSV file that matches the cell values from the Crop Management Scenario raster to a particular crop type. • User indicates the function that will be used to estimate yield. 	<ul style="list-style-type: none"> • The tool produces yield estimates through one of three yield functions for each pixel of the Crop Management Scenario raster. • A raster is produced by the tool representing the yield (in tons per ha) on each pixel from the Crop Management Scenario raster.

3.2.4. Habitat Quality

The GeoApp's Habitat Quality widget produces raster images of relative habitat quality within an area of interest for a particular species. The giant anteater (*Myrmecophaga tridactyla*) is a vulnerable species with a geographic range that extends through Mato Grosso state (Miranda et al., 2014b). Given that it is threatened by elements such as road networks and human agricultural activities that are dominant throughout the AOI, we chose to use the GeoApp's Habitat Quality widget to model the giant anteater's relative habitat quality within the AOI. To do so, we used land cover rasters from the beginning (i.e., 2000) and conclusion (i.e., 2005) of the Morton et al. (2006) analysis period (Table 1 provides a general description of model inputs and outputs). Both rasters were obtained from the *MapBiomass Project* and were reclassified to indicate areas of habitat and non-habitat for the giant anteater. Two "threat rasters" were used to indicate the location of roads and agricultural operations, both of which are significant threats the species faces (Miranda et al., 2014b). The species' sensitivity to each threat was provided to the model in CSV files. Sensitivity values within the CSV files were chosen after experimenting with a range of values in an effort to accurately reflect relative threats to the giant anteater.

3.2.5. Crop Production

To assess the productivity of the land identified in Morton et al. (2006) as converted to agriculture, we used the GeoApp's Crop Production widget. This widget requires the user to provide a "Crop Management Scenario" raster where the crop(s) of interest are geo-located to raster cells (Table 1). Each crop of interest is indicated within the raster dataset with a unique identifier, beginning with 1 and increasing by a value of 1 for each additional crop of interest. All other raster cells are coded to 0. We created such a raster by presuming that all land clearings from Morton et al. were converted to soybean production. A CSV file was used by the model to match cell values from the Crop Management Scenario raster to yield information for soybeans. This yield information was provided through the United Nations Food and Agriculture Organization (FAO) and sub-national datasets for a host of commonly-grown crops and were adjusted according to regional climatic conditions (see Monfreda et al., 2008 for more detail). The final output from our model run provided information on soybean yield (in tons per hectare) for each land conversion pixel within the AOI.

3.3. Results

The Telecoupling GeoApp assists in exploring the effects of interactions between sending, receiving, and spillover systems. Here we report on land conversion and its ecological impacts in the Brazilian Amazon. While Morton et al. (2006) did not explicitly mention Chinese soybean

demand as a driver of the land clearings in the AOI, international demand, including demand from China, certainly motivates Brazilian land conversion (Nepstad et al., 2006; Jenkins, 2012; Silva, 2017). Thus, we believe the results reported below can be viewed as the telecoupling effects produced by interactions between the receiving system (i.e., China) and the sending system (i.e., Brazil).

The Change Detection widget provides a visual understanding of land conversion within the AOI. Figure 7 focuses on an individual zone within the center of the AOI. The magenta areas are those where vegetative cover was reduced during the period extending from December 31, 1999 to December 31, 2004, and many of these areas correspond to the same cropland deforestation clearings identified by Morton et al. (2006). In terms of promoting sustainability, this widget helps to address targets such as halting deforestation by the year 2020 and ensuring the sustainable use of terrestrial ecosystems, both of which were described in the UN Sustainable Development Goals (Goal 15 – Life on Land).

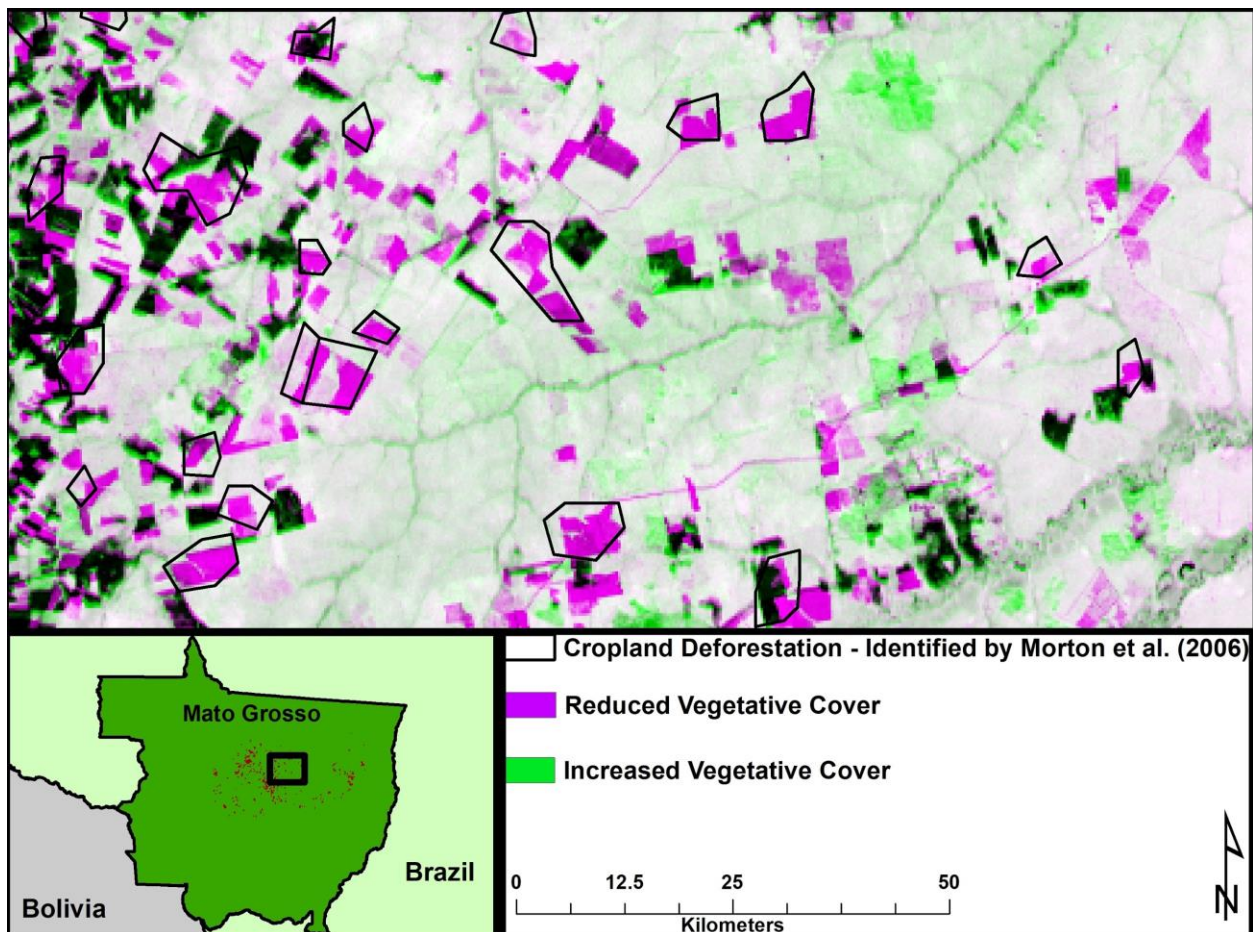


Figure 7. Land change detection from December 31, 1999 to December 31, 2004. *Note:* The land conversion image was produced using the GeoApp’s Change Detection widget. This image was then imported to ArcMap to add the inset map, legend, and north arrow.

These land clearings have an ecological impact on systems near and far. Global geophysical processes are altered as carbon is released into the atmosphere following the conversion of forested land to agriculture. We assessed above-ground carbon stock degradation within the AOI by isolating the land clearings from Morton et al. (2006) and applying the GeoApp's Forest Carbon Edge Effect tool, which found that the land cleared was a sink for 43,584,168 megagrams (Mg) of carbon (to provide perspective, South American agrosilvicultural operations have been found to hold between 39 and 102 Mg of carbon per hectare (Albrecht and Kandji, 2003)). Figure 8 indicates where the land conversion took place and the amount of carbon per plot that had been sequestered. In this figure, the land clearing polygons are overlaid on top of the 2000 land cover image to offer some context for the clearings. This reveals that most land conversion took place near land that had already been converted to pasture or agricultural operations by 2000. Understanding the amount of carbon sequestered within forested plots significantly assists in integrating climate change measures with national policies and is critical to ensuring the conservation of terrestrial ecosystems, the former being an indicator of UN Sustainable Development Goal 13 (Climate) while the latter relates to Goal 15.

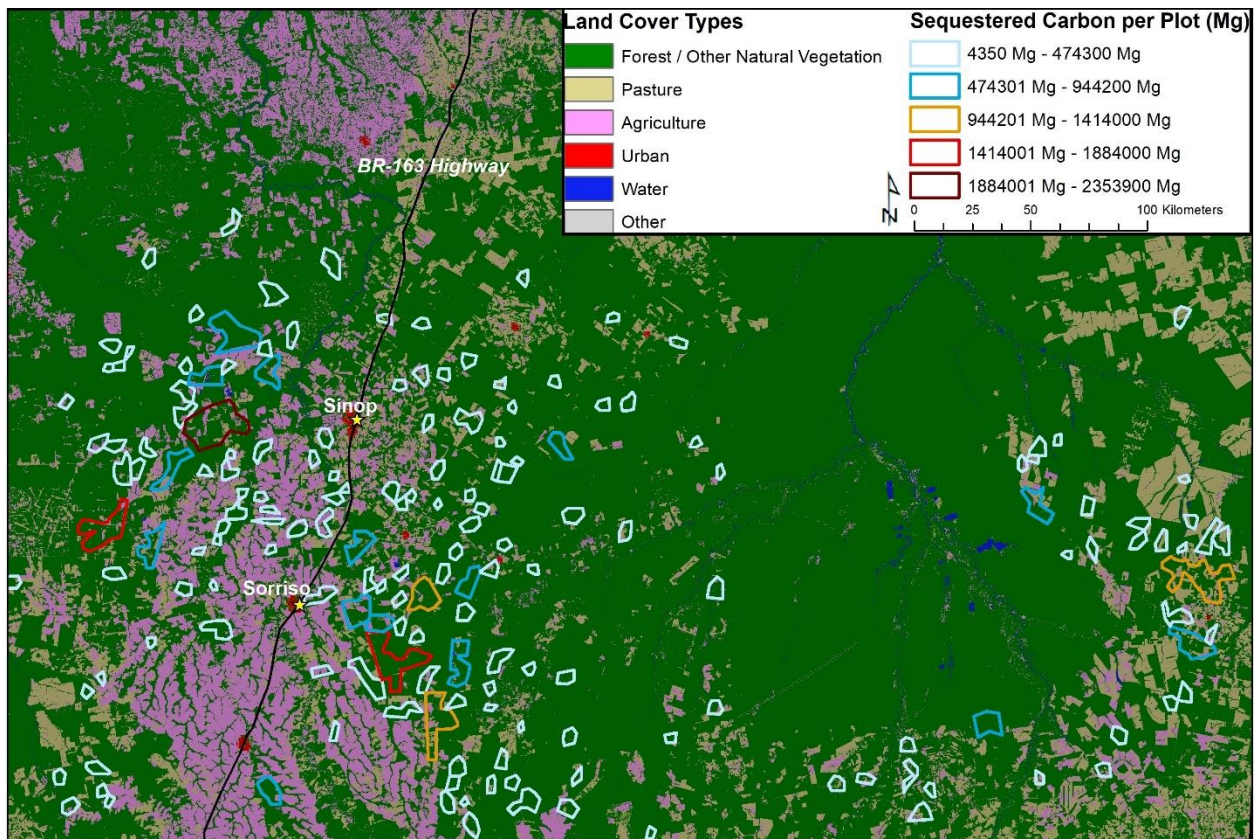


Figure 8. Carbon that had been sequestered by each land clearing plot. *Note:* The amount of carbon sequestered per pixel was calculated using the GeoApp's Forest Carbon Edge Effect widget. Pixel values were aggregated for each land clearing plot in ArcMap. The legend, north arrow, plot symbology, and map features (i.e., road and cities) were also added in ArcMap.

Agricultural expansion puts biodiversity at risk. We assessed the quality of habitat for the giant anteater within the AOI at the beginning and conclusion of the Morton et al. (2006) study period. This analysis contributes to efforts to reduce the degradation of natural habitats and halt the loss of biodiversity (i.e., UN Sustainable Development Goal 15). Using the GeoApp's Habitat Quality tool we produced two habitat quality rasters (one for the year 2000, the other for 2005) designating habitat quality on a scale of 0 (not habitable) to 1 (most suitable habitat) for each pixel. The mean pixel value for the year 2000 habitat quality raster was 0.71, while the mean pixel value for the year 2005 was 0.60. Investigating pixels where the change from 2000 to 2005 was at least a 0.05 increase or decrease in suitability, we find that 77% of cells exhibited no change in suitability (or the change in suitability was within the range of -0.05 to 0.05), 21% exhibited a decrease in suitability, and habitat suitability improved in 2% of cells. Figure 9 identifies where these changes in habitat quality took place.

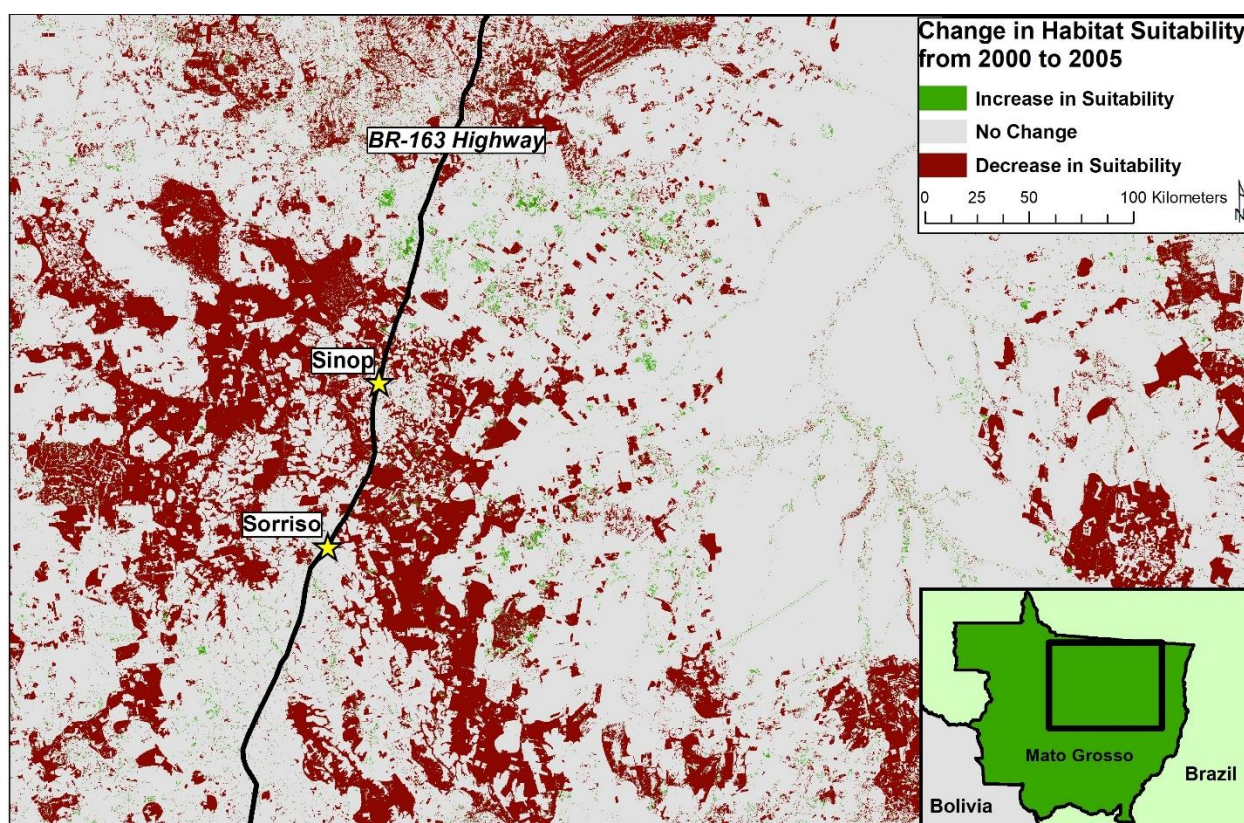


Figure 9. Change in giant anteater habitat quality from 2000 to 2005. *Note:* Habitat suitability for the years 2000 and 2005 were evaluated using the GeoApp's Habitat Quality tool. ArcMap was used to calculate locations where suitability increased and decreased. ArcMap was also used to adjust symbology, add the inset map, legend, north arrow, and map features (i.e., road and cities).

Finally, bringing new land under production improves food security and economic growth. The Crop Production analysis found that the total amount of land in the AOI brought under cultivation from 2000 to 2004 was slightly more than 3 million hectares. From this newly cultivated land the model estimated an average yield of 3.34 tons per hectare, which exceeded the state of Mato Grosso's average yield of 2.96 tons per hectare from 2000 to 2009 (Arvor et al., 2012). These findings are critical to several targets for achieving food security described in UN Sustainable Development Goal 2.

4. Discussion

The telecoupling framework seeks to advance understandings of socioeconomic and environmental interactions between coupled human and natural systems across distances. How these interactions influence global sustainability is of particular interest to researchers and decision makers alike. We have provided a telecoupling case study - soybean trade between Brazil and China - and used the GeoApp to analyze carbon sequestration, habitat quality, and agricultural production outcomes from these interactions.

We acknowledge that by using the Mato Grosso land clearing plots from Morton et al. (2006; see Figure 5) rather than gathering primary data directly intended to explore the Brazil-China telecoupling, we are unable to identify the destination of soy grown on these plots with absolute certainty. However, because Mato Grosso is the largest producer and exporter of Brazilian soybeans (Lopes et al., 2017) and because Morton et al. (2006) were able to establish a relationship between agricultural extensification and soy commodity prices, it is reasonable to assume that some, if not all, of the soy produced on these plots was ultimately sent abroad, primarily to China. By making use of secondary data to explore the effects of land conversion, we demonstrate a major strength of the GeoApp: users equipped with a research question can gain a breadth of knowledge regarding telecoupling processes and sustainability outcomes solely using pre-existing datasets. The barriers to entry, which are low given that no software needs to be installed, remain low since use of the web GIS platform is not contingent on users collecting their own data through fieldwork operations.

Further, we acknowledge that while the telecoupling framework identifies sending, receiving, and spillover systems (see the Introduction section), both the receiving and spillover systems received little attention in the Brazil-China soybean telecoupling case study. This speaks both to the current set of geoprocessing widgets in the GeoApp and the way in which the investigation has been framed. While widget development is ongoing, the GeoApp's current set of geoprocessing tools are more suited for evaluating ecological and land change outcomes than they are suited for social outcomes. Brazil has experienced an array of ecological outcomes as a result of growing agricultural extensification and intensification in recent decades; thus, for this

case study, we were able to highlight more widgets by focusing on the sending system. Had the focus of the case study been on the receiving system, a suite of widgets that, among other things, quantify economic development, which has not yet been developed, and produce food security metrics, which is in the development stage, would be useful. In terms of incorporating spillover systems, the GeoApp provides visualization capabilities in its Add Systems and Upload Systems From Table widgets. However, whether the web application is able to offer a robust set of widgets to inspect the elements of a spillover system ultimately depends on the questions asked by the application user and the capacities of the widgets that are provided. As it relates to the Brazil-China telecoupling case study, it is important to keep in mind that we asked questions largely through a bilateral lens (thus directing attention away from spillover systems), with a greater emphasis on environmental and land change outcomes (thus directing attention toward the sending system).

Using the GeoApp we found that the Brazil-China soybean telecoupling leads to negative environmental effects within the sending system. As the urgency to confront climate change grows and the challenges to taking meaningful climate action become more apparent, understandings of the global effects of large-scale deforestation become important from both a policy making and stakeholder engagement perspective. We found that the land cleared in the AOI for crop cultivation had been acting as a sink for 43.5 million Mg of carbon. Note that this value pertains only to above-ground carbon pools, it does not account for below-ground, soil, or standing dead matter pools. Site-specific carbon density values were obtained from the literature, and we encourage the reader to review the NatCap InVEST user guide for a detailed explanation of the model (Sharp et al., 2017).

We also found land clearings to be detrimental to biodiversity. The AOI occupies approximately 235,580 km², of which 44,770 km² became unsuitable to our species of interest, the giant anteater, from 2000 to 2005. Further, the Mato Grosso dry forest, which spans through the AOI, provides critical habitat for many species, including the giant anteater, as it reaches from the Amazon biome in the north to the Cerrado biome in the south. Therefore, while the giant anteater was the species of interest in our analysis, the land clearings within the AOI have broad biodiversity implications given the large number of endemic species within this unique habitat and the role these forests play in migratory patterns.

In spite of these negative environmental effects, the telecoupling analysis also highlighted the yield potential of the area cleared for production. Approximately 30,000 km² (or 3,000,000 hectares) were cleared from the AOI from 2000 to 2004, giving way to land capable of producing 3.3 tons of soybean per hectare and thus demonstrating both positive and negative potentials of the Brazil-China soybean telecoupling. The broader sustainability question posed by the soybean telecoupling, or at least one such question, therefore becomes: how can soybean demand from the receiving system, which has implications for human well-being, be sustainably

met by the sending system so as to avoid damaging global environmental consequences? The answer to this question will be critical to the stewardship of resources facing increased pressure from human activities.

4.1. Future Work: Sustainable Development

The GeoApp offers an integrated platform to study the components of human-nature interactions while avoiding software installation procedures and licenses. As the world becomes increasingly interconnected and concern grows regarding the global implications of seemingly routine activities, such as commodity trade and resource extraction, a web application with low barriers to entry, like the GeoApp, can play an important role advancing global sustainability objectives and engaging stakeholders.

For instance, the agenda set by the UN's Sustainable Development Goals seeks to address global issues related to human well-being (e.g., ending poverty and ensuring prosperity) and environmental sustainability (e.g., promoting clean energies and responsibly managing terrestrial and aquatic resources). As we demonstrated in the Results section, a user of the GeoApp can explore deforestation or biodiversity loss, and in the process make contributions to Sustainable Development Goal 15: "Sustainably manage forests, combat desertification, halt and reverse land degradation, and halt biodiversity loss." Similarly, progress toward goals 9 and 13 - "Build resilient infrastructure, promote sustainable industrialization, and foster innovation" and "Take urgent action to combat climate change and its impacts", respectively - can be made using the GeoApp's widget for calculating CO₂ emissions from the flow of goods. Equipped with this knowledge, policy makers and researchers can communicate the externalities of trade and better coordinate sustainable industrial development initiatives. While we presented results related to soybean yield and area of production, at its current stage of development the GeoApp is better suited for addressing those Sustainable Development Goals oriented toward environmental management initiatives.

To balance environmental goals with other research arenas, we are currently in the process of integrating a set of widgets that take a deeper look at development goals related to food security, among other topics. One of these soon-to-be-integrated widgets calculates the lower limit of energy requirement (LLER) in kilocalories per day for a particular area of interest, which the user provides in the form of a shapefile. WorldPop provides spatially explicit age structure data in five-year age groupings at a 1-km resolution for all locations in Latin America, Africa, and Asia (Tatem et al., 2013; data are available for download at www.worldpop.org). The GeoApp widget isolates the total number of people per pixel in each age grouping within the defined area of interest and applies a set of equations established by the FAO to calculate LLER (see FAO, 2008). Figure 10 shows the output of an early version of this widget for Shanshan County in western China with the number of kilocalories per day needed to satisfy each age grouping given

in the column titled “Lower Limit of Energy Requirement.” The total number of individuals within each age grouping in Shanshan County is given in the column titled “Population.” This information would be valuable to decision-makers seeking to improve food security within particularly vulnerable locations and help make progress concerning Sustainable Development Goal 2: “End hunger, achieve food security, and improved nutrition and promote sustainable agriculture.”

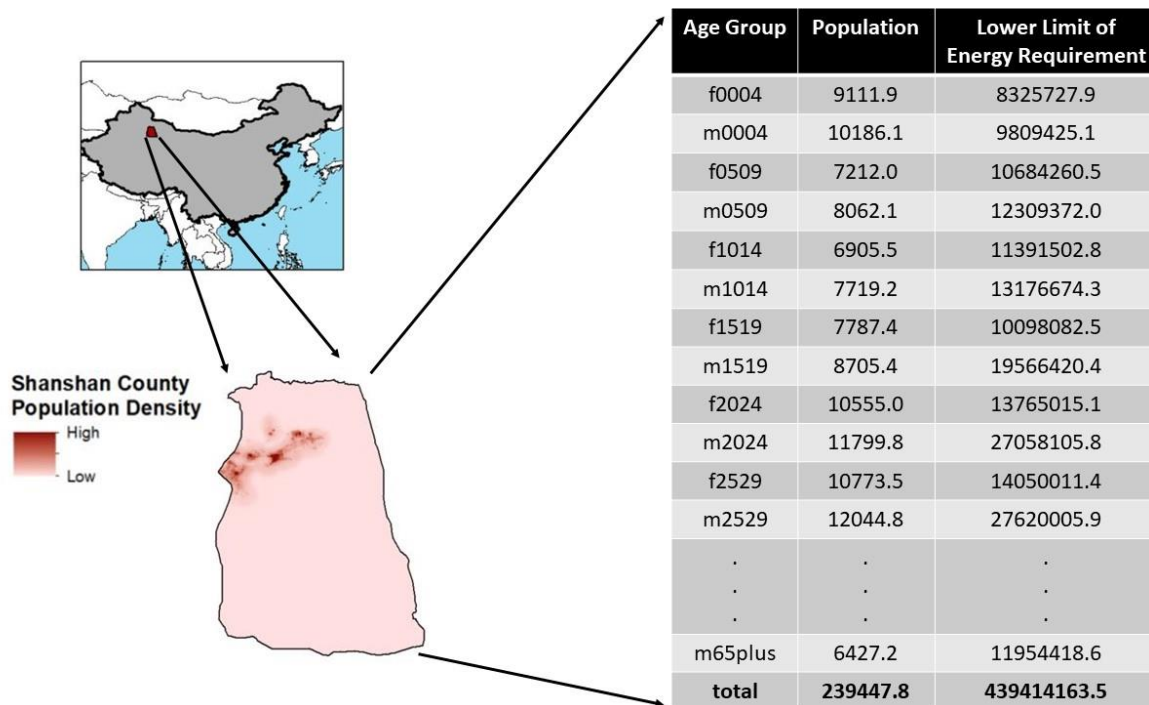


Figure 10. The population and lower limit of energy requirement (in kilocalories per day) for each five-year age grouping in Shanshan County, China. *Note:* “Age Group” field refers to the five-year age groupings for each sex. Therefore, f0004 refers to the female 0-4 age group, while m0004 refers to the male 0-4 age group, and so on. The output in the table was produced using the GeoApp’s Nutrition Metrics tool and has been reformatted to comply with space limitations.

Additionally, ongoing efforts to address sustainable development challenges using the GeoApp include explicit framings of the widgets that most closely align with a particular telecoupling and an explanation of how these widgets address Sustainable Development Goals. For example, a user of the GeoApp might be interested in the global production of fertilizers and the effect that fertilizer availability at multiple locations may have on rivers, lakes, and streams. Supplied documentation would inform the user of widgets they may find useful for their analysis. In this case, Draw Radial Flows, Nutrient Delivery Ratio, and Crop Production may be useful. Additionally, a list of Sustainable Development Goals – and their accompanying targets – that the telecoupling analysis might help to address would be supplied to the user, such as SDG 6 “Clean Water and Sanitation”, SDG 14 “Life Below Water”, and SDG 15 “Life on Land.” We

expect this enhancement of the GeoApp to encourage users to understand how the various elements of the analyzed telecoupling influence long-term efforts to fight poverty, end hunger, reduce resource exploitation, and address climate change, among other critical goals.

5. Conclusion

In this article, we introduced the Telecoupling GeoApp (available at <https://telecoupling.msu.edu/geo-app>), a web GIS application that operationalizes the systems, agents, flows, causes, and effects of the telecoupling framework. The GeoApp is part of a larger collection of software and applications called the Telecoupling Toolbox. All source code, sample data, and documentation of the tools and applications within the Telecoupling Toolbox are available at <https://msu-csis.github.io/telecoupling-toolbox/>. The development of the telecoupling framework was motivated by a need to understand the dramatic changes resulting from system interactions across scales and distances. Similarly, development of the GeoApp was motivated by a need to better visualize and quantify these interactions, as well as recognition that sustainability goals would be best met if low-barrier analysis resources were available to researchers, policy makers, and stakeholders seeking to understand the effects of system interactions. The GeoApp provides a suite of widgets capable of representing the agents, systems, and flows of a telecoupling as well as widgets to visualize and quantify the causes and effects of a telecoupling, which are particularly valuable when addressing sustainability concerns or targets of sustainable development (such as those provided by the UN Sustainable Development Goals).

We described the Brazil-China soybean telecoupling and used the GeoApp to investigate some effects, particularly those arising in the sending system. We found that land cleared to meet the receiving system's soybean demand removed forest cover from the sending system that had been playing an important role both in sequestering carbon and providing valuable biodiversity habitat. On the other hand, we discovered the land that was ultimately put into production had a yield potential that was 0.3 tons per hectare higher for soybeans than the average potential in the state of Mato Grosso, thus signifying the challenges of balancing environmental concerns with the need to feed an expanding global population.

Efforts to address sustainable development will need to identify optimal strategies that work toward a number of diverse targets and that do not sacrifice one goal in one location for the sake of achieving another goal in a separate location. This will not be easy, particularly given the complexity of global systems and the challenges of disentangling ever-present telecouplings. It is our hope that the GeoApp will offer a valuable resource to make sense of a multifaceted,

interconnected world and provide a means to confront increasingly complex sustainability challenges.

6. Acknowledgements

Funding from the National Science Foundation (grant number 1518518) and Michigan AgBioResearch is gratefully acknowledged. We would also like to acknowledge the MapBiomass project (mapbiomass.org), WorldPop (www.worldpop.org.uk), and the Natural Capital Projects's InVEST program (<https://www.naturalcapitalproject.org/invest/>) which provided data and analysis modules for the study. Finally, we acknowledge the helpful comments from two anonymous reviewers, as well as suggestions and revisions offered by Sue Nichols.

7. References

Adger, W.N., Barnett, J., Brown, K., Marshall, N., & O'Brien, K. (2013). Cultural dimensions of climate change impacts and adaptation. *Nature Climate Change*, 3, 112-117. <http://dx.doi.org/10.1038/nclimate1666>.

Albrecht, A., & Kandji, S.T. (2003). Carbon sequestration in tropical agroforestry systems. *Agriculture, Ecosystems and Environment*, 99(1-3), 15-27. [https://doi.org/10.1016/S0167-8809\(03\)00138-5](https://doi.org/10.1016/S0167-8809(03)00138-5).

Amazon AWS. (2017). Amazon Web Services. Available at <https://aws.amazon.com>. [Accessed on December, 2017].

Arvor, D., Meirelles, M., Dubreuil, V., Begue, A., & Shimabukuro, Y.E. (2012). Analyzing the agricultural transition in Mato Grosso, Brazil, using satellite-derived indices. *Applied Geography*, 32(2), 702-713. <https://doi.org/10.1016/j.apgeog.2011.08.007>.

Brannstrom, C., Jepson, W., Filippi, A.M., Redo, D., Xu, Z., & Ganesh, S. (2008). Land change in the Brazilian savanna (Cerrado), 1986-2002: Comparative analysis and implications for land-use policy. *Land Use Policy*, 25(4), 579-595. <https://doi.org/10.1016/j.landusepol.2007.11.008>.

Car, N.J., Christen, E.W., Hornbuckle, J.W., & Moore, G.A. (2012). Using a mobile phone short messaging service (SMS) for irrigation scheduling in Australia – farmers' participation and utility evaluation. *Computers and Electronics in Agriculture*, 84, 132-143. <https://doi.org/10.1016/j.compag.2012.03.003>.

Carter, N.H., Vina, A., Hull, V., McConnell, W.J., Axinn, W., Ghimire, D., & Liu., J. (2014). Coupled human and natural systems approach to wildlife research and conservation. *Ecology and Society*, 19(3), 43. <http://dx.doi.org/10.5751/ES-06881-190343>.

Chaplin-Kramer, R., Ramler, I., Sharp, R., Haddad, N.M., Gerber, J.S., West, P.C., Mandle, L., Engstrom, P., Baccini, A., Sim, S., Mueller, C., & King, H. (2015). Degradation in carbon stocks near tropical forest edges. *Nature Communications*, 6, 10158. <http://dx.doi.org/10.1038/ncomms10158>.

DeFries, R.S., Rudel, T., Uriarte, M., & Hansen, M. (2010). Deforestation driven by urban population growth and agricultural trade in the twenty-first century. *Nature Geoscience*, 3, 178-181. <http://dx.doi.org/10.1038/ngeo756>.

Deines, J.M., Liu, X., & Liu, J. (2016). Telecoupling in urban water systems: An examination of Beijing's imported water supply. *Water International*, 41(2), 251-270. <http://dx.doi.org/10.1080/02508060.2015.1113485>.

Dou, Y., Silva, R.F.B., Yang, H., & Liu, J. *In Press*. Spillover effect offsets the conservation effort in the Amazon. *Journal of Geographical Sciences*.

FAO. (2008). FAO methodology for the measurement of food deprivation: Updating the minimum dietary energy requirements. Food and Agriculture Organization of the United Nations, Rome, Italy.

FAO. (2017). FAOSTAT. Available at <https://www.fao.org/faostat/en/#home>. [Accessed on December, 2017].

ESRI. (2017). ESRI's Living Atlas of the World. Available at <https://livingatlas.arcgis.com>. [Accessed on December, 2017].

Fernside, P.M. (1997). Greenhouse gases from deforestation in Brazilian Amazonia: Net committed emissions. *Climatic Change*, 35(3), 321-360. <https://doi.org/10.1023/A:1005336724350>.

Foley, J.A., DeFries, R., Asner, G.P., Barford, C., Bonan, G., Carpenter, S.R., Chapin, F.S., Coe, M.T., Daily, G.C., Gibbs, H.K., Helkowski, J.H., Holloway, T., Howard, E.A., Kucharik, C.J., Monfreda, C., Patz, J.A., Prentice, I.C., Ramankutty, N., & Snyder, P.K. (2005). Global consequences of land use. *Science*, 309(5734), 570-574. <http://dx.doi.org/10.1126/science.1111772>.

Fu, P., & Sun, J. (2010). *Web GIS: Principles and Applications*. Redlands, CA: ESRI Press.

Gasparri, N.I., Kuemmerle, T., Meyfroidt, P., de Waroux, Y., & Kreft, H. (2016). The emerging soybean production frontier in southern Africa: Conservation challenges and the role of south-south telecouplings. *Conservation Letters*, 9(1), 21-31. <http://dx.doi.org/10.1111/conl.12173>.

Geist, H.J., & Lambin, E.F. (2002). Proximate causes and underlying driving forces of tropical deforestation. *BioScience*, 52(2), 143-150. [https://doi.org/10.1641/0006-3568\(2002\)052\[0143:PCAUDF\]2.0.CO;2](https://doi.org/10.1641/0006-3568(2002)052[0143:PCAUDF]2.0.CO;2).

Godfray, H.C.J., Beddington, J.R., Crute, I.R., Haddad, L., Lawrence, D., Muir, J.F., Pretty, J., Robinson, S., Thomas, S.M., & Toulmin, C. (2010). Food security: The challenge of feeding 9 billion people. *Science*, 327(812), 812-818. <http://dx.doi.org/10.1126/science.1185383>.

Goldsmith, P. (2008). Soybean production and processing in Brazil. In, *Soybeans: Chemistry, Production, Processing, and Utilization* (pp. 773-798). AOCS Press, Champaign, IL, USA. <http://dx.doi.org/10.1016/B978-1-893997-64-6.50024-X>.

Huete, A.R. (1988). A soil-adjusted vegetation index (SAVI). *Remote Sensing of Environment*, 25(3), 295-309. [https://doi.org/10.1016/0034-4257\(88\)90106-X](https://doi.org/10.1016/0034-4257(88)90106-X).

Jenkins, R. (2012). China and Brazil: Economic impacts of a growing relationship. *Journal of Current Chinese Affairs*, 41(1), 21-47.

Kareiva, P., Tallis, H., Ricketts, T.H., Daily, G.C., & Polasky, S. (2011). *Natural Capital: Theory and Practice of Mapping Ecosystem Services*. Oxford University Press, Oxford, UK.

Kasischke, E.S., Turetsky, M.R., Ottmas, R.D., French, N.H.F., Hoy, E.E., & Kane, E.S. (2008). Evaluation of the composite burn index for assessing fire severity in Alaskan black spruce forests. *International Journal of Wildland Fire*, 17(4), 515-526. <https://doi.org/10.1071/WF08002>.

Kates, R.W., Clark, W.C., Corell, R., Hall, J.M., Jaeger, C.C., Lowe, I., McCarthy, J.J., Schellnhuber, H.J., Bolin, B., Dickson, N.M., Faucheux, S., Gallopin, G.C., Grubler, A., Huntley, B., Jager, J., Jodha, N.S., Kaspersen, R.E., Mabogunje, A., Matson, P., Mooney, H., Moore, B., O'Riordan, T., & Svedin, U. (2001). Sustainability science. *Science*, 292(5517), 641-642. <http://dx.doi.org/10.1126/science.1059386>.

Komiyama, H., & Takeuchi, K. (2006). Sustainability science: Building a new discipline. *Sustainability Science*, 1(1), 1-6. <http://dx.doi.org/10.1007/s11625-006-0007-4>.

Kramer, D., Hartter, J. Boag, A., Jain, M., Stevens, K., Nicholas, K.A., McConnell, W.J., & Liu, J. (2017). Top 40 questions in coupled human and natural systems (CHANS) research. *Ecology and Society*, 22(2), 44. <https://doi.org/10.5751/ES-09429-220244>.

Lambin, E.F., & Meyfroidt, P. (2011). Global land use change, economic globalization, and the looming land scarcity. *Proceedings of the National Academy of Sciences*, 108(9), 3465-3472. <http://dx.doi.org/10.1073/pnas.1100480108>.

Liu, J., Hull, V., Batistella, M., DeFries, R., Dietz, T., Fu, F., Hertel, T.W., Izaurrealde, R.C., Lambin, E.F., Li, S., Martinelli, L.A., McConnell, W.J., Moran, E.F., Naylor, R., Ouyang, Z., Polenske, K.R., Reenberg, A., Rocha, G., Simmons, C.S., Verburg, P.H., Vitousek, P.M., Zhang, F., & Zhu, C. (2013). Framing sustainability in a telecoupled world. *Ecology and Society*, 18(2), 26. <http://dx.doi.org/10.5751/ES-05873-180226>.

Liu, J. (2014). Forest sustainability in China and implications for a telecoupled world. *Asia & the Pacific Policy Studies*, 1(1), 230-250. <http://dx.doi.org/10.1002/app5.17>.

Liu, J., Mooney, H., Hull, V., Davis, S.J., Gaskell, J., Hertel, T., Lubchenco, J., Seto, K.C., Gleick, P., Kremen, C., & Li, S. (2015a). Systems integration for global sustainability. *Science*, 347(6225). <http://dx.doi.org/10.1126/science.1258832>.

Liu, J., Hull, V., Luo, J., Yang, W., Liu, W., Vina, A., Vogt, C., Xu, Z., Yang, H., Zhang, J., An, L., Chen, X., Li, S., Zhiyun, O., Xu, W., & Zhang, H. (2015b). Multiple telecouplings and their complex interrelationships. *Ecology and Society*, 20(3), 44. <http://dx.doi.org/10.5751/ES-07868-200344>.

Liu, J., Yang, W., & Li, S. (2016). Framing ecosystem services in the telecoupled Anthropocene. *Frontiers in Ecology and the Environment*, 14(1), 27-36. <http://dx.doi.org/10.1002/16-0188.1>.

Liu, J. (2017). Integration across a metacoupled world. *Ecology and Society*, 22(4), 29. <https://doi.org/10.5751/ES-09830-220429>.

Lopes, H.S., Lima, R.S., Leal, F., & Nelson, A.C. (2017). Scenario analysis of Brazilian soybean exports via discrete event simulation applied to soybean transportation: The case of Mato Grosso State. *Research in Transportation Business & Management*, 25, 66-75. <http://dx.doi.org/10.1016/j.rtbm.2017.09.002>.

McFeeters, S.K. (1996). The use of normalized difference water index (NDWI) in the delineation of open water features. *International Journal of Remote Sensing*, 17(7), 1425-1432. <https://doi.org/10.1080/01431169608948714>.

Millenium Ecosystem Assessment. (2005). *Ecosystems and Human Well-Being: Biodiversity Synthesis*. World Resources Institute, Washington, DC.

Miranda, S., Bustamante, M., Palace, M., Hagen, S., Keller, M., & Ferreira, L.G. (2014a). Regional variations in biomass distribution in Brazilian savanna woodland. *Biotropica*, 46(2), 125-138. <http://dx.doi.org/10.1111/btp.12095>.

Miranda, F., Bertassoni, A., & Abba, A.M. (2014b). *Myrmecophaga tridactyla*, the IUCN Red List of Threatened Species 2014. Available at <http://dx.doi.org/10.2305/IUCN.UK.2014-1.RLTS.T14224A47441961.en>. [Accessed on December 2017].

Monfreda, C., Ramankutty, N., & Foley, J.A. (2008). Farming the planet: 2. Geographic distribution of crop areas, yields, physiological types, and net primary production in the year 2000. *Global Biogeochemical Cycles*, 22(1). <http://dx.doi.org/10.1029/2007GB002947>.

Morton, D.C., DeFries, R.S., Shimabukuro, Y.E., Anderson, L.O., Arai, E., Espirito-Santo, F., Freitas, R., & Morisette, J. (2006). Cropland expansion changes deforestation dynamics in the southern Brazilian Amazon. *Proceedings of the National Academy of Sciences*, 103(39), 14637-14641. <http://dx.doi.org/10.1073/pnas.0606377103>.

Mueller, N.D., Gerber, J.S., Johnston, M., Ray, D.K., Ramankutty, N., & Foley, J.A. (2012). Closing yield gaps through nutrient and water management. *Nature*, 490, 254-257. <http://dx.doi.org/10.1038/nature11420>.

Nepstad, D.C., Stickler, C.M., & Almeida, O.T. (2006). Globalization of the Amazon soy and beef industries: Opportunities for conservation. *Conservation Biology*, 20(6), 1595-1603. <http://dx.doi.org/10.1111/j.1523-1739.2006.00510.x>.

Ostrom, E. (2009). A general framework for analyzing sustainability of social-ecological systems. *Science*, 325(419). <http://dx.doi.org/10.1126/science.1172133>.

Peters, D.P.C., Groffman, P.M., Nadelhoffer, K.J., Grimm, N.B., Collins, S.L., Michener, W.K., & Huston, M.A. (2008). Living in an increasingly connected world: A framework for continental-scale environmental science. *Frontiers in Ecology and the Environment*, 6(5), 229-237. <http://dx.doi.org/10.1890/070098>.

Polsky, C., Neff, R., & Yarnal, B. (2007). Building comparable global change vulnerability assessments: The vulnerability scoping diagram. *Global Environmental Change*, 17(3-4), 472-485. <https://doi.org/10.1016/j.gloenvcha.2007.01.005>.

Richards, P.D., Myers, R.J., Swinton, S.M., & Walker, R.T. (2012). Exchange rates, soybean supply response, and deforestation in South America. *Global Environmental Change*, 22(2), 454-462. <https://doi.org/10.1016/j.gloenvcha.2012.01.004>.

Sachs, J.D. (2012). From millennium development goals to sustainable development goals. *Lancet*, 379(9832), 2206-2211. [http://dx.doi.org/10.1016/S0140-6736\(12\)60685-0](http://dx.doi.org/10.1016/S0140-6736(12)60685-0).

Sharp, R., Tallis, H.T., Ricketts, T., Guerry, A.D., Wood, S.A., Chaplin-Kramer, R., Nelson, E., Ennaanay, D., Wolny, S., Olwero, N., Vigerstol, K., Pennington, D., Mendoza, G., Aukema, J., Foster, J., Forrest, J., Cameron, D., Arkema, K., Lonsdorf, E., Kennedy, C., Verutes, G., Kim, C.K., Guannel, G., Papenfus, M., Toft, J., Marsik, M., Bernhardt, J., Griffin, R., Glowinski, K., Chaumont, N., Perelman, A., Lacayo, M., Mandel, L., Hamel, P., Vogl, A.L., Rogers, L., Bierbower, W., Denu, D., & Douglass, J. (2017). *INVEST VERSION 3.3.3. User's Guide*. The Natural Capital Project, Stanford University, University of Minnesota, The Nature Conservancy, and World Wildlife Fund.

Silva, R.F.B., Batistella, M., Dou, Y., Moran, E., Torres, S.M., & Liu, J. (2017). The Sino-Brazilian telecoupled soybean system and cascading effects for the exporting country. *Land*, 6(53). <http://dx.doi.org/10.3390/land6030053>.

Singels, A., & Smith, M.T. (2006). Provision of irrigation scheduling advice to small-scale sugarcane farmers using a web-based crop model and cellular technology: A South African case study. *Irrigation and Drainage*, 55(4), 363-372. <http://dx.doi.org/10.1002/ird.231>.

Stern, N. (2008). The economics of climate change. *The American Economic Review*, 98(2), 1-37. <http://www.jstor.org/stable/29729990>

Sun, J., Wu, W., Tang, H., & Liu, J. (2015). Spatiotemporal patterns of non-genetically modified crops in the era of expansion of genetically modified food. *Nature Scientific Reports*, 5(14180). <http://dx.doi.org/10.1038/srep14180>.

Sun, J., Yu-xin, T., & Liu, J. (2017). Telecoupled land-use changes in distant countries. *Journal of Integrative Agriculture*, 16(2), 368-376. [http://dx.doi.org/10.1016/S2095-3119\(16\)61528-9](http://dx.doi.org/10.1016/S2095-3119(16)61528-9).

Tatem, A.J., Garcia, A.J., Snow, R.W., Noor, A.M., Gaughan, A.E., Gilbert, M., & Linard, C. (2013). Millennium development health metrics: Where do Africa's children and women of childbearing age live? *Population Health Metrics*, 11, 11. <https://doi.org/10.1186/1478-7954-11-11>.

Tonini, F., & Liu, J. (2017). Telecoupling toolbox: Spatially explicit tools for studying telecoupled human and natural systems. *Ecology and Society*, 22(4), 11. <https://doi.org/10.5751/ES-09696-220411>.

Tuan, F.C., Fang, C., & Cao, Z. (2004). China's soybean imports expected to grow despite short-term disruptions. Electronic Outlook Report from the Economic Research Service, United States Department of Agriculture (USDA).

Turner, B.L., Kasperson, R.E., Meyer, W.B., Dow, K.M., Golding, D., Kasperson, J.X., Mitchell, R.C., & Ratick, S.J. (1990). Two types of global environmental change: Definitional and spatial-scale issues in their human dimensions. *Global Environmental Change*, 1(1), 14-22. [https://doi.org/10.1016/0959-3780\(90\)90004-S](https://doi.org/10.1016/0959-3780(90)90004-S).

Turner, B.L., Kasperson, R.E., Matson, P.A., McCarthy, J.J., Corell, R.W., Christensen, L., Eckley, N., Kasperson, J.X., Luers, A., Martello, M.L., Polsky, C., Pulsipher, A., & Schiller, A. (2003). A framework for vulnerability analysis in sustainability science. *Proceedings of the National Academy of Sciences*, 100(14), 8074-8079. <http://dx.doi.org/10.1073/pnas.1231335100>.

Turner, B.L., Lambin, E.F., & Reenberg, A. (2007). The emergence of land change science for global environmental change and sustainability. *Proceedings of the National Academy of Sciences*, 104(52), 20666-20671. <http://dx.doi.org/10.1073/pnas.0704119104>.

United Nations. (2016). *Global Sustainable Development Report 2016*. Department of Economic and Social Affairs, New York, NY.

Vitousek, P.M. (1992). Global environmental change: An introduction. *Annual Review of Ecology and Systematics*, 23, 1-14. <https://doi.org/10.1146/annurev.es.23.110192.000245>.

Vörösmarty, C.J., McIntyre, P.B., Gessner, M.O., Dudgeon, D., Prusevich, A., Green, P., Glidden, S., Bunn, S.E., Sullivan, C.A., Liermann, C.R., & Davies, P.M. (2010). Global threats to human water security and river biodiversity. *Nature*, 467, 555-561. <http://dx.doi.org/10.1038/nature09440>

Warnken, P.F. (1999). *The Development and Growth of the Soybean Industry in Brazil*. Iowa State University Press, Ames, IA, USA.

Zeppel, H. (2008). Education and conservation benefits of marine wildlife tours: Developing free-choice learning experiences. *The Journal of Environmental Education*, 39(3), 3-18. <http://dx.doi.org/10.3200/JOEE.39.3.3-18>.